Initial Design of a Real-Time and an Intershot Bolometric Data Exploitation Strategy for DTT

E. Peluso[1,2], G. M. Apruzzese[1], A. Belpane[3], S. Palomba[4], L. Senni[5], E. Giovannozzi[1] , V. D'Agostino[2], T. Craciunescu[6], M. Gelfusa[2], P. Gaudio[2] and L. Boncagni[1]

(1) ENEA, Nuclear Department, C.R. ENEA-Frascati, Via E. Fermi 45, 00044, Frascati (RM), Italy (2) Department of Industrial Engineering, University of Rome, Via del Politecnico 1, 00133, Rome(RM) , Italy
(3)Consorzio RFX (CNR, ENEA, INFN, Università di Padova, Acciaierie Venete SpA), Corso Stati, Padova, 35127, Italy, (4) DTT S.C.a r.l., Via E. Fermi 45, I-00044, Frascati (RM), Italy
(5) National Institute for Laser, Plasma and Radiation Physics, Magurele-Bucharest, Romania, (5) CNR - Institute for applied mathematics 'Mauro Picone' (IAC)Via dei Taurini, 19, 00185 - Roma – Italy

emmanuele.peluso@enea.it ; emmanuele.peluso@uniroma2.it

Background:

The Divertor Tokamak Test (DTT) Facility is an experiment under construction at the ENEA Research Centre in Frascati; its main mission is to test the power extraction strategies for the first nuclear fusion power plant [1].
Currently, a Phase1, a Phase2 and a Phase3 are planned, with different implemented diagnostics and with increased external heating (~19MW, ~28MW and ~45MW respectively[2]).
A preliminary conceptual design of the bolometric diagnostic, requiring 216 lines of sight (LoS), has been completed [3]. The bolometers will be housed in a pinhole box support unit [4]; the thermo-mechanical analysis can be found in [5] instead. Synthetic profiles (phantoms) were considered to validate the overall layout by adapting an expectation maximisation algorithm for a maximum likelihood (ML) approach[6].

DTT

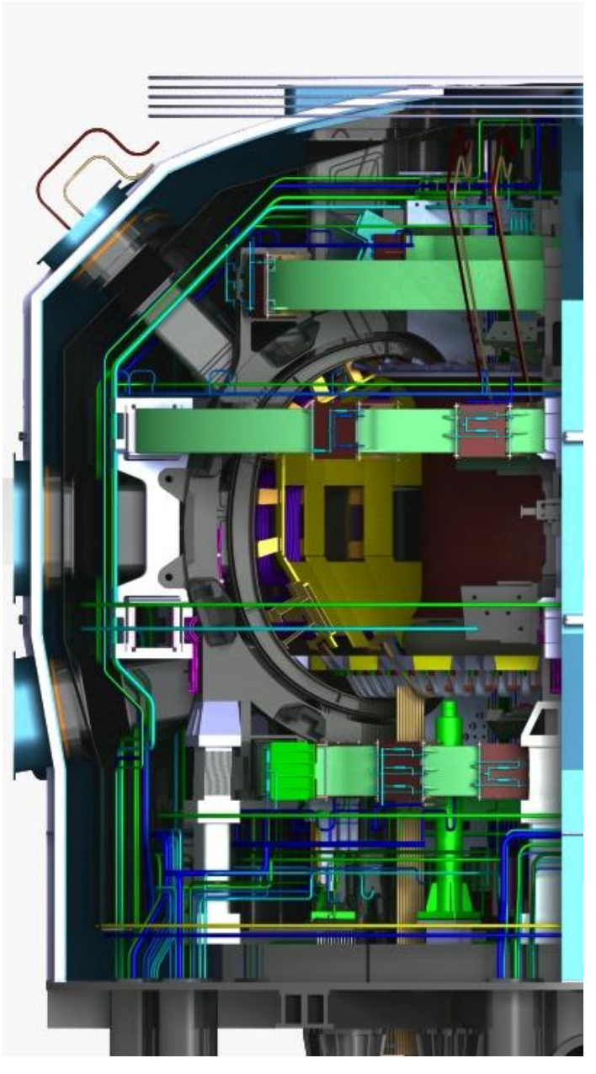

R [m]	2.19
a [m]	0.70
I_P [MA]	5.5
B_T [T]	5.85
P_{tot} [MW]	45
Pulse length [s]	100

For Single Null (SN), Flat-Top, Full Power Scenario
$T_e \sim 10\ keV$
$n_e \sim 2 \cdot 10^{20}\ m^{-3}$

Main features of the ML approach implemented

- The variance associated with the reconstructed emissivity and hence the uncertainties in the derived quantities can be obtained [7];
- an anisotropic smoothing has been implemented that can take into account differently oriented directional derivatives for smoothing[8];
- the width of each LoS is considered and both the etendue and the contribution of each truncated pyramidal voxel are estimated[6].

Objectives of this contribution

Describe the designs or current state of the art of strategies for estimating:
A) the radiated power of the plasma, P_{rad}, using directly arrays of Line Integrals (L.I) for a Real Time (RT) implementation;
B) P_{rad} in different regions of the plasma, using Region of Interest (ROIs) in RT for feedback control;
C) tomograms from a ML approach during the inter-shot phase to provide more accurate estimates of P_{rad} in different locations of the device as well as radiation profiles

Estimation of P_{rad} from arrays of L.I in RT *(A objective)*

Starting from the absorbed power from a detector, P_m, the L.I or I_m , can be derived for a bolometer m, i.e. :

$$P_m = \sum_{p}^{\#\,voxel} \left(\varepsilon_p dV_p d\Omega_p\right)_m = \frac{E_m}{4\pi} I_m \Rightarrow I_m = \sum_{p}^{\#\,voxel} H_{mp}\varepsilon_p = \int \varepsilon(r,\theta)\, dl_m$$

where ε is the synthetic emissivity profile described by a phantom; p stands for a truncated pyramidal voxel, seen by the detector with etendue E, with a volume dV and emitting by an infinitesimal solid angle $d\Omega$ towards the bolometer. The radiated power P_j inside the vacuum vessel can be derived from an array of q bolometers (i.e. P1, P2 or P3) by a weighted sum of the L.I:

$$P_j = 2\pi \mathrm{R}_0 \sum_{q}^{\#\,L.I.} S_{qj} \left(\frac{I_{qj}}{L_{qj}}\right) c_j$$

Where the length of each LoS is L and the poloidal section of the LoS is S

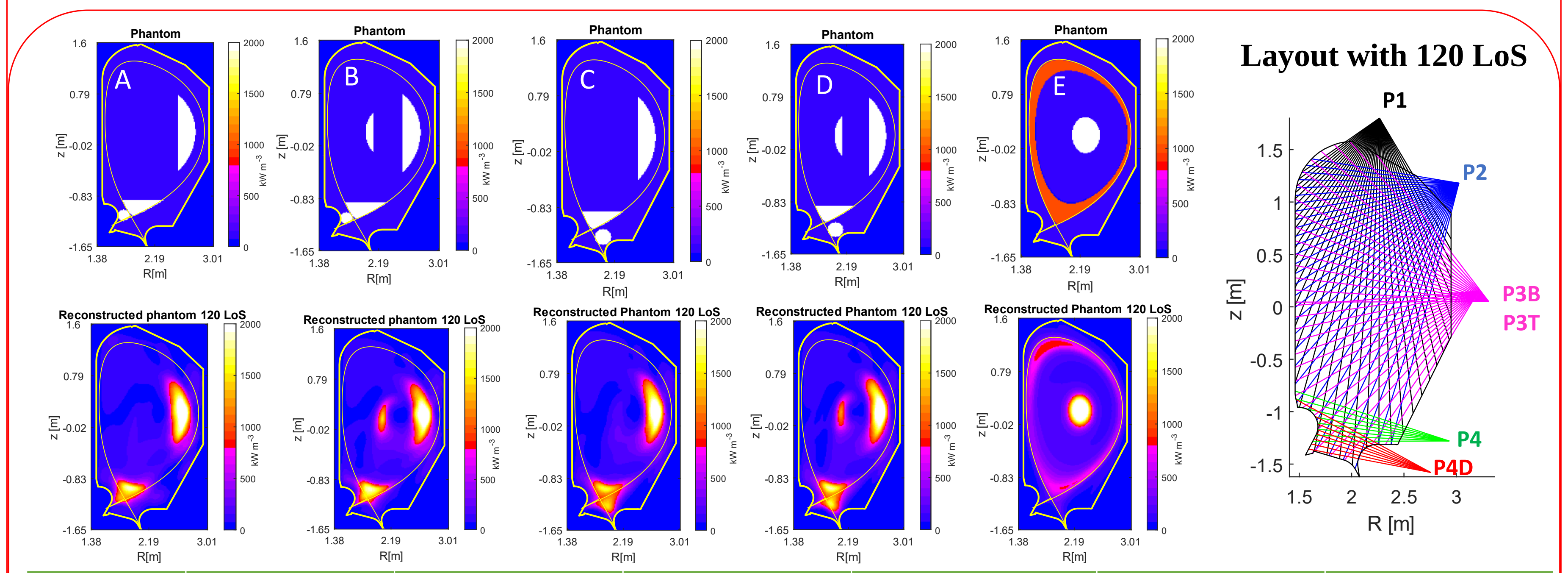

Layout with 120 LoS

Phantom		ML		Array P1		Array P2		Array P3		P1 and P2		P1,P2 and P3	
	P_{rad} $[MW]$	P_{rad} $[MW]$	$\epsilon_{\%}$	P_{rad} $[MW]$	$\delta_{\%}$	P_{rad} $[MW]$	$\delta_{\%}$	P_{rad} $[MW]$	$\delta_{\%}$	P_{rad} $[MW]$	$\delta_{\%}$	P_{rad} $[MW]$	$\delta_{\%}$
A	13.44	13.43	11.0	12.96	−3.92	13.72	1.86	14.18	5.06	13.34	−0.94	13.62	1.14
B	14.63	14.62	10.0	14.49	−0.86	14.96	2.26	15.18	3.69	14.73	0.72	14.87	1.73
C	13.93	13.91	9.6	13.32	−4.55	14.00	0.54	14.49	3.87	13.66	−1.95	13.93	0.070
D	15.13	15.15	8.5	14.79	−2.35	15.22	0.48	15.48	2.16	15.00	−0.91	15.16	0.12
E	16.72	16.41	3.2	18.59	11.72	15.62	−5.15	14.30	−14.77	17.10	4.02	16.17	−1.52

Where ϵ stands for the percentage error estimated using the ML approach from a set of projections with normal added Gaussian noise[6]; δ stands for the discrepancy in percentage between the L.I estimates of P_{rad} and the expected one.

Estimation of P_{rad} from ROIs for RT feedback control *(B objective)*

The RT feedback control of the radiation pattern for prevention is a delicate matter.
In seeding experiments, an unstable X-point radiator could lead to a Multifaceted Asymmetric Radiation From the Edge (MARFE) [9] and then to a so-called density limit disruption. Another example of a possible perturbation pathway would be the growth and dynamics of Tearing Modes (TM), which have recently been linked to impurity fluxes and their accumulation[10][11].
A wise approach would be to monitor not only the total radiated power, but also the power radiated from different regions of the device. A fast, but approximate method can be found in [12]. Here it has been adapted for DTT by defining the following closed system composed of eight initial ROIs.

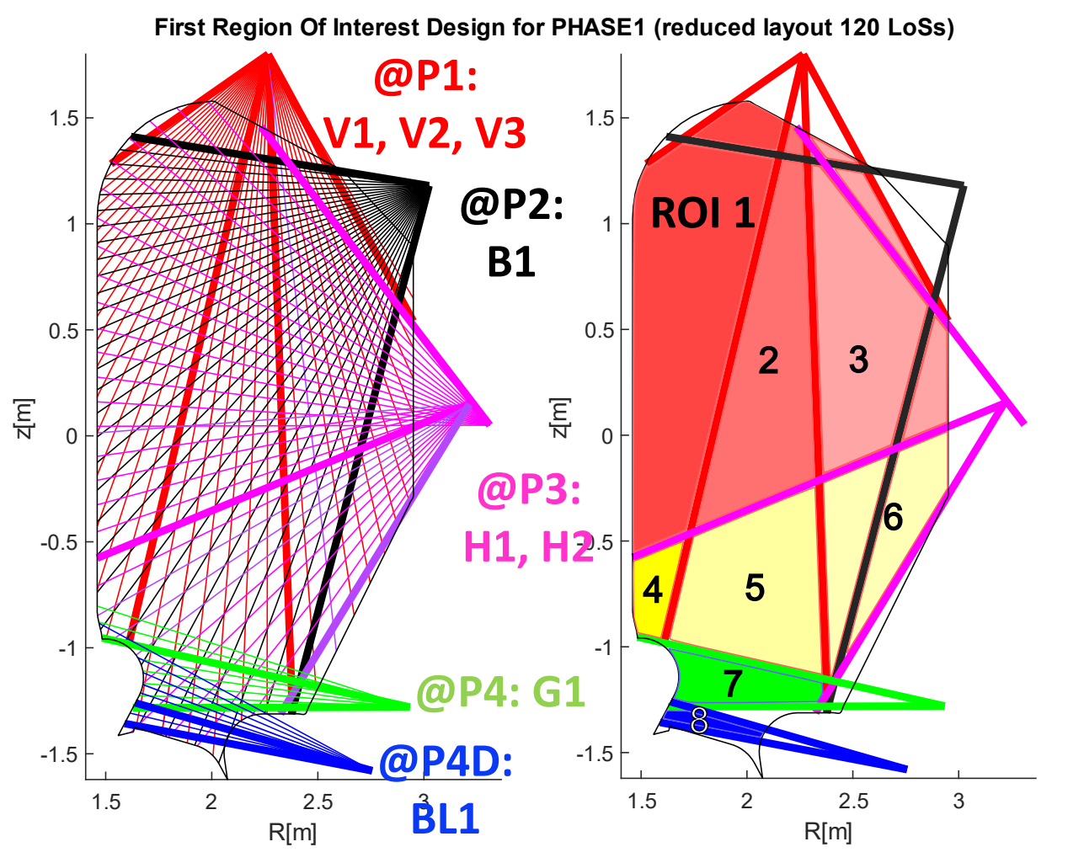

Measurements	ROIs #
V1	1,4
V2	2,5,7,8
V3	3,6
H1	1,2,3
H2	4,5,6,7,8
P4	7
P4D	8
B1	1,2,3,4,5,6,7,8

$$\begin{cases} V_1 = 2\pi R_0 \displaystyle\sum_{q}^{\#\,L.I.\in V1} S_q \left(\frac{I_q}{L_q}\right) = \frac{S_{ROI1}}{S_{V1}} P_{\mathrm{ROI1}} + \frac{S_{ROI4}}{S_{V1}} P_{\mathrm{ROI4}} \\ \qquad \cdots \\ B1 = 2\pi R_0 \displaystyle\sum_{q}^{\#\,L.I.\in B1} S_q \left(\frac{I_q}{L_q}\right) = \sum_{r}^{8} \frac{S_{ROI\,r}}{S_{B1}} P_{ROI\,r} \end{cases} \Rightarrow \begin{pmatrix} V_1 \\ V_2 \\ V_3 \\ H_1 \\ H_2 \\ G_1 \\ BL_1 \\ B1 \end{pmatrix} = \mathbb{G} \begin{pmatrix} P_{ROI1} \\ P_{ROI2} \\ P_{ROI3} \\ P_{ROI4} \\ P_{ROI5} \\ P_{ROI6} \\ P_{ROI7} \\ P_{ROI8} \end{pmatrix}$$

The matrix $\mathbb{G}$ contains the imposed geometric weights representing the fraction of the poloidal areas for each ROI. Using a non-negative least-squares fit, the radiated power $P_{ROI1,\dots,8}$ in each region can be estimated in RT.

P_{rad} from ML tomograms for intershot analysis *(C objective)*

The error-free estimation of the ML code can in principle run in RT, as it is based on standard low-dimensional matrix computations [13]; however, such an option could in principle lead to a possible misuse of the results.
A better approach would be to optimise the algorithm and implement a layered code, including a GUI, for inter-shot analysis aimed at providing tomograms and the derived quantities with their uncertainties from the ML approach.

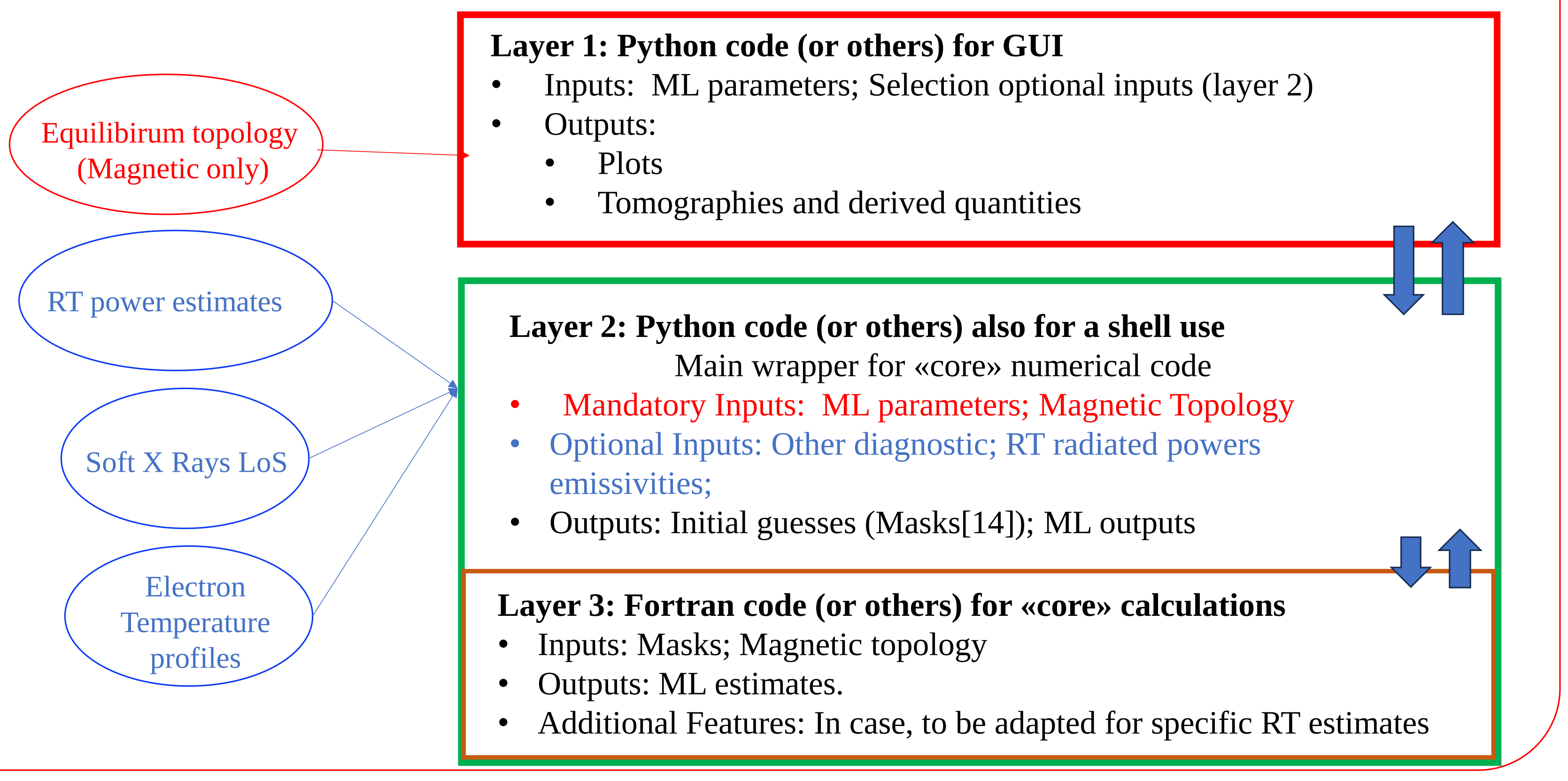

Equilibirum topology (Magnetic only)

RT power estimates

Soft X Rays LoS

Electron Temperature profiles

Layer 1: Python code (or others) for GUI
- Inputs: ML parameters; Selection optional inputs (layer 2)
- Outputs:
  - Plots
  - Tomographies and derived quantities

Layer 2: Python code (or others) also for a shell use
Main wrapper for «core» numerical code
- Mandatory Inputs: ML parameters; Magnetic Topology
- Optional Inputs: Other diagnostic; RT radiated powers emissivities;
- Outputs: Initial guesses (Masks[14]); ML outputs

Layer 3: Fortran code (or others) for «core» calculations
- Inputs: Masks; Magnetic topology
- Outputs: ML estimates.
- Additional Features: In case, to be adapted for specific RT estimates

Work in progress (STAY TUNED!)

1. The designed strategies need to be extensively tested on different configurations (SN, X-Divertor and Negative Triangularity) and mimicking some time slices of a pulse with phantoms.
2. Efforts must be made to:
   a. obtain a consolidated set of weights (c_j) by studying more synthetic profiles;
   b. both study and further define a layout of the ROIs for RT, also taking into account a possible modification of the layout for Phase 1;
   c. realise the described inter-shot analysis tool and build the actual interfaces with CODAS.

References and Acknowledgment

[1] F. Romanelli 2024 Nuclear Fusion. IOP Publishing on behalf of the IAEA
[2] F. Crisanti, G. Giruzzi and P. Martin, 2024, DIVERTOR TOKAMAK TEST facility Research Plan
[3]G. M. Apruzzese, submitted to 50th EPS Conference, Salamanca, Spain (08th-12th July 2024)
[4] A. Belpane, ICFDT7, Frascati, Italy,(21st-28th October 2024)
[5] V. D'Agostino 33rd SOFT, Dublin, Ireland (22nd -27th September 2024)
[6] E. Peluso, 33rd SOFT, Dublin, Ireland (22nd -27th September 2024)
[7] T. Craciunescu et al., 2018, Rev. Sci. Instrum. 89,053504, https://doi.org/10.1063/1.5027880
[8] T. Craciunescu et al, 2023 Phys. Scr. 98 125603 https://doi.org/10.1088/1402-4896/ad081e
[9] M. Bernert et al. Nuclear Materials and Energy 34 (2023) 101376
[10] G. Pucella et al. Nucl. Fusion 61 (2021) 046020 (12pp)
[11] S.Zeng et al., Nucl. Fusion 63 (2023) 046018 (12pp)
[12] R. Rossi et al. Matter Radiat. Extremes 8, 046903 (2023)
[13] H.H. Barrett, et al., I. Theory, Phys. Med. Biol. 39, 833–846 (1994).
[14]E.Peluso et al, 2022, Plasma Phys. Control. Fusion 64 045013, https://doi.org/10.1088/1361-6587/ac4854

Authors are grateful to:
Antonio Castaldo (ENEA), Lori Gabelleri (DTT), Matteo Iafrati (ENEA)

DTT Consortium (DTT S.C.a r.l. Via E. Fermi 45 I-00044 Frascati (Roma) Italy)